

## URBAN LAND-USE AND POLLUTION IMPACTS ON MESOSCALE CIRCULATIONS OVER HOUSTON

Gustavo Carrió\*, W. R. Cotton  
Colorado State University, Fort Collins, Colorado

### 1. INTRODUCTION

The objective of this study is to investigate the effects of the growth of the Houston metropolitan area on the characteristics and intensity of convection and precipitation. For this purpose, we implemented the Town Energy Budget (TEB) urban model into Regional Atmospheric Modeling System (RAMS@CSU; Cotton et al, 2003). The microphysical package can consider the explicit activation of cloud nucleating aerosols (Saleeby and Cotton, 2004). The National Land Cover Data (NLCD) for the Houston area corresponding to the years 1992, 2001 and 2006 were used for an objective experimental design of the land-use sensitivity experiments. We analyzed the impact on two distinct groups of convective cells triggered by the sea breeze circulation on August 24 2000. The first group of storms occurred southeast of the city and was not influenced by the urban aerosols, while the second, was and occurred north of the city (downwind) a few hours later. The effect of land-use on convection and precipitation was dramatic for the storms SE of the city and it was linked to a monotonic increase in the intensity of the sea breeze. The total volume of precipitation increased monotonically 9, 11, and 30% (over a run with no city) for 1992, 2001, and 2006 NLCD land use datasets, respectively. As expected, the convective cells downwind of the city were invigorated by a greater latent heat release linked to higher amounts of liquid water transported to supercooled levels. However, precipitation did not show a monotonic behavior when we varied the intensity of the urban aerosol sources. When further increasing aerosol concentrations, the collision mechanisms involved in the rapid liquid-ice phase change became less efficient, a greater fraction of condensate was transported out through the storm outflow, and therefore the precipitation efficiency was reduced.

---

Corresponding author's address: Gustavo G. Carrió, Atmospheric Science Department, Atmospheric Science Bldg., Colorado State University, Fort Collins CO 80523, USA; e-mail: [carrio@atmos.colostate.edu](mailto:carrio@atmos.colostate.edu)

### 2. MODEL CONFIGURATION AND EXPERIMENTAL DESIGN

These mesoscale sensitivity experiments were performed using RAMS@CSU with three two-way interactive nested grids with 42 vertical levels and horizontal grid spacing of 15, 3.75, and 0.75 km. The corresponding domain sizes were: 1065 X 915km, 382.5 X 382.5km, and 151.5 X 151.5km, respectively, and centered over the city of Houston. Grids 1 and 2 were used to simulate the synoptic and mesoscale environments, while grid 3 was used to resolve deep convection as well as the sea-breeze circulation. The location of the grids is given in Fig. 1.

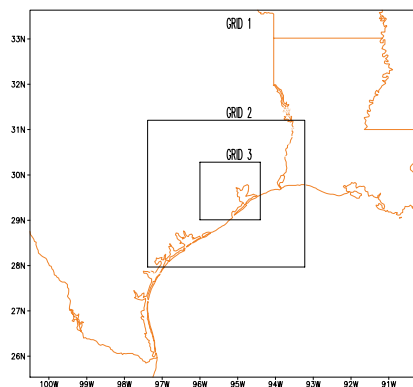


**Figure 1.** Grid configuration.

The vertical grid was stretched using with 75m spacing at the finest levels to provide better resolution within the first 1.5 km, and the model top extended to approximately 20 km above ground level. All simulations were heterogeneously initialized with 40 km ETA data from 24 July 2000 at 00:00 UTC and the simulation period was 24h. The mixing ratios and number concentrations of all water species (cloud droplets, drizzle drops, rain, pristine ice, snow, aggregates, graupel and hail) were predicted. Cloud-nucleating aerosols were also considered as prognostic variables. The RAMS@CSU code has been modified to initialize the different grids with NLCD data. These data (available at a pixel size of ~30m) allow a much better representation of the land

surface heterogeneities and their sub-grid area fractions of the various land-use categories considered by the model. We considered numerical experiments using the 1992, 2001, and 2006 land-use satellite data sets as well as *NO CITY* run. The latter corresponds to the satellite data closest to the case used for this study (2001), but the urban sub-grid patches were replaced by the predominant land-use categories in the city surroundings. To choose aerosol concentrations representative of a highly polluted day, we analyzed two aerosol data sets documented during TexAQS-GoMACCS:CCN measurements on the CIRPAS Twin Otter and NOAA P-3 along with other data collected by the Ronald H. Brown data for Houston and various locations of the gulf area. Peak CCN concentrations exceeded  $30000\text{cm}^{-3}$ , however, we eventually used lower CCN concentrations. A series of preliminary tests indicated that increasing the latter above  $4000\text{cm}^{-3}$  did not produce a significant impact on the results. City aerosol sources were considered by nudging these high concentrations at the first model level above the ground multiplied by the sub-grid urban fraction of the corresponding grid cell. In addition to high CCN concentrations over the city, we initialized the surroundings and the gulf area with more moderate and cleaner values, respectively. GCCN concentrations were not varied in these numerical experiments. They were initialized using O'Dowd et al (1997) formulae for sea-salt concentrations over the gulf and lower concentrations over land. The numerical experiments corresponding to results presented in this abstract are shown in Table I. The city CCN concentrations listed in this table corresponded to the maximum values (entirely urban grid cell) nudged at the first model level to consider CCN sources.

**Table I: Numerical experiments.**

Land use	CCN concentrations ( $\text{cm}^{-3}$ )		
	City	rural	Gulf
1992	1000, 2000, 4000	500	200
2001	1000, 2000, 4000	500	200
2006	1000, 2000, 4000	500	200
NO CITY	500		200

### 3. RESULTS

In this series of sensitivity experiments, two distinct groups of convective cells were simulated. The location of these two groups is given in figure 2 that compares the spatial distribution of accumulated precipitation for the entire simulation period, to those corresponding to two time intervals.

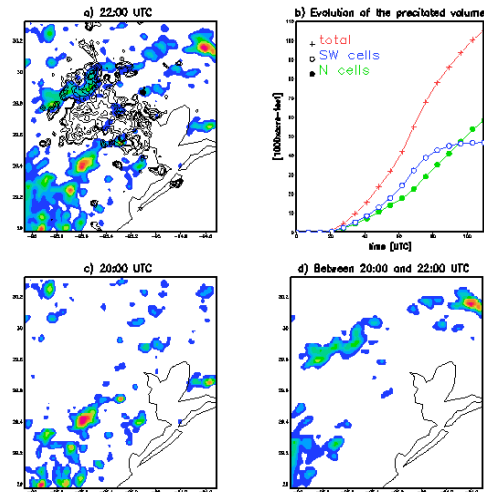


**Figure 2.** Accumulated precipitation for the entire simulation period, and for the periods ending at 20:00 UTC and between 20:00 and 22:00 UTC (a, c, and d, respectively). Evolution of the integral precipitated volume for each group of cells and for both (b).

These results correspond to the numerical experiment that should be more representative for this case (2001 satellite data and  $2000\text{cm}^{-3}$  sources). The first group of storms occurred southwest of the city between 16:00 and 20:00 UTC (SW cells) while the second, north of the urban area and between 20:00 and 22:00 UTC (N cells). This figure also compares the time evolution of the precipitated volume for each group (2b). The N cells were within the simulated plume of pollutants as the prevailing wind was SSE. Conversely, the SW cells were virtually not affected by the urban sources of aerosol. Figure 3 compares the averaged precipitation rates and accumulated values derived from radar data to those simulated for the same run. The SW cells as well as the most intense N cells are indicated in this figure. The domain-averaged precipitation rates and accumulated values simulated for 2001 satellite data and  $2000\text{cm}^{-3}$  sources were slightly higher than those observed. However, the temporal evolution and the location of the most intense cells are very similar.

First we compare the runs corresponding to 1992, 2001, and 2006 satellite data as well as the *NO CITY* run. As seen in Fig. 4, the SW cells occurred outside the aerosol plume. The shaded area represents CCN concentrations at least 10% above the background values one hour before the convective activity develops (approximately 17:00 UTC) and the contours denote the position of these cells. As expected, the numerical experiments varying only the intensities of these aerosol sources exhibited negligible differences for the SW cells (not shown).

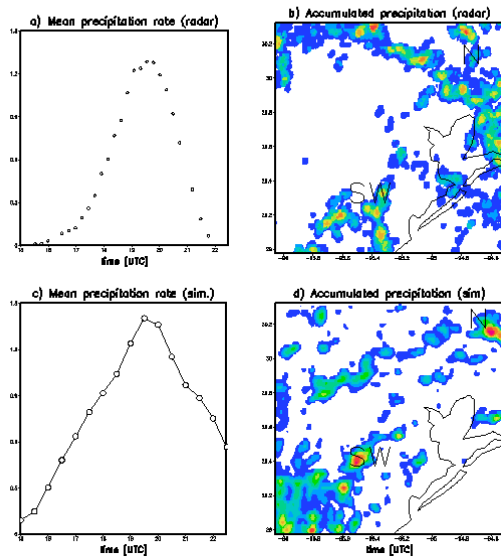


**Figure 3.** Comparison of the grid-averaged precipitation rates and accumulated values derived from radar data to those simulated.

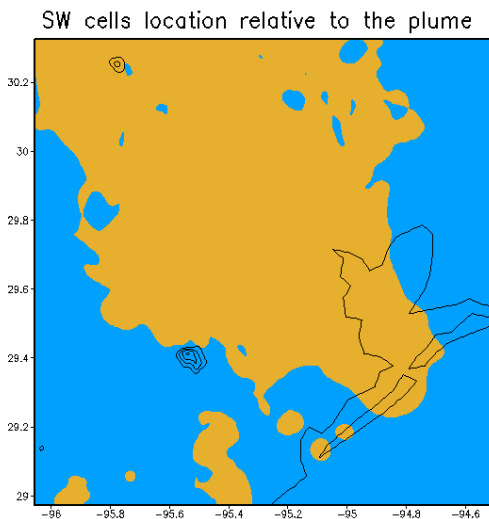


**Figure 4.** Shading represents the aerosol plume one hour before the convective activity. The contours indicate the position of the SW cells ( $2001, 2000 \text{ cm}^{-3}$ ).

However, increasing the size of the city had a great impact on the total volume of precipitation (Fig. 5a). Differences up to 25% were simulated for the total volume precipitated over the finest grid (grid 3). Maximum precipitation rates were 50, 40, and 20% higher than the NO CITY run for the 2006, 2001, and 1992 cities, respectively (not shown). Figure 5b is analogous to Fig 5a but only for urban gridcells. For the urban area, differences in precipitated volume were positive only for the 2001 and 2006 runs.

When comparing 1992, 2001, 2006, and NO CITY runs, the maximum simulated updrafts

were comparable, although the area covered by convective cells increased with increasing city size. The probability density functions of vertical motions are compared in Fig. 6a, b for the same set of runs. Although maximum values were comparable, updrafts greater than  $5 \text{ ms}^{-1}$  were more frequent for experiments considering larger urban areas. The evolution of the total precipitated volume and the area with precipitation is compared for the same set of sensitivity runs in Figs. 6c and d, respectively.

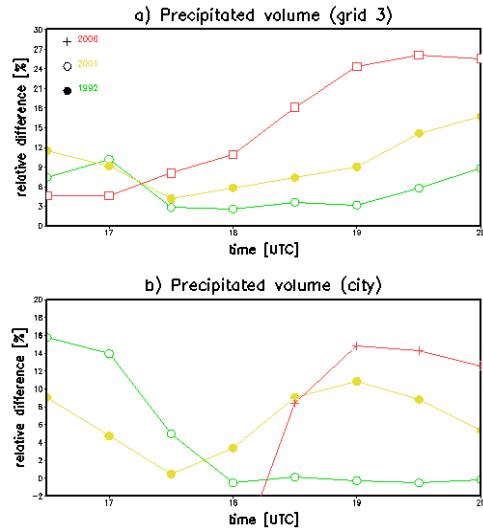


**Figure 5.** Comparison total precipitated volume for grid 3 (a) and for the urban area (b) for 1992, 2001, and 2006 cities.

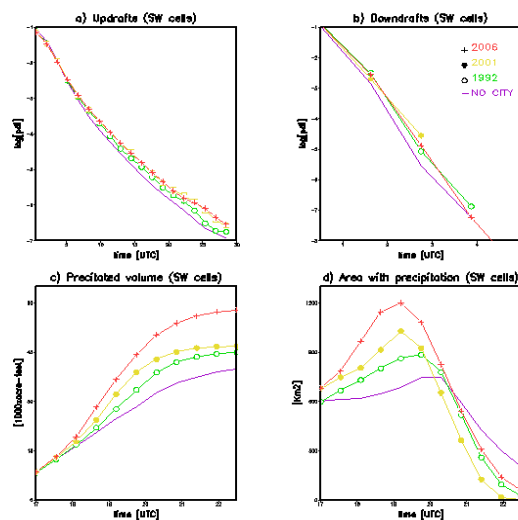


**Figure 6.** Probability density functions for vertical motions (a and b) for experiments varying city size. Total precipitated volume and area with precipitation in panels c and d, respectively

The total precipitated volume monotonically increased with increasing city size (up almost

60%). The area with precipitation behaved in a similar manner with slightly higher relative increases. Therefore, the area-averaged precipitation rates did not change significantly and the increase in the precipitated volume was mainly linked to the increase in the storm size. Maximum liquid and ice water paths (LWP and IWP, respectively) simulated for 1002, 2001, and 2006 were higher than those of the NO CITY run, however the response was not monotonic (not shown).

Conversely, the group of convective cells that occurred north of the city between 20:00 and 22:00 UTC showed a very distinct behavior. As seen in Fig 7, considering larger cities (with no aerosol sources) produced no monotonic changes and almost no regularities in vertical motions, precipitation rates and total volumes, and water paths. However, it must be noted that the maximum area covered by these cells was between 700 and 800km<sup>2</sup> for 1992, 2001, and 2006 cities, while it was above 1200km<sup>2</sup> for the NO CITY run.

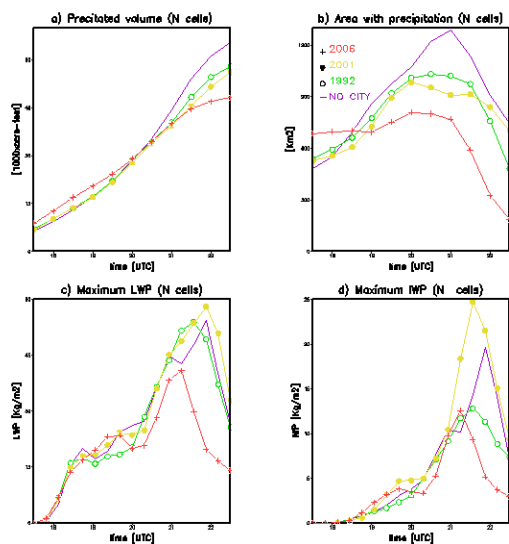


**Figure 7.** Comparison of precipitated volume, area with precipitation, and maximum water paths for experiments varying city size.

The remarkably different response of the SW cells may be explained by a significant intensification of the sea-breeze where they occurred. As seen in Fig 8, the intensity of the sea-breeze (~ SE) increases monotonically for larger urban areas. The SE flux averaged over first 1000m is given in Figs 8b, c, and d for 1992, 2001, and 2006 land use, respectively. These fluxes were computed at a simulation time that corresponds to one hour prior to the most intense convective activity (19:30 UTC); the position of the cells at the latter time is given in Fig. 8a.

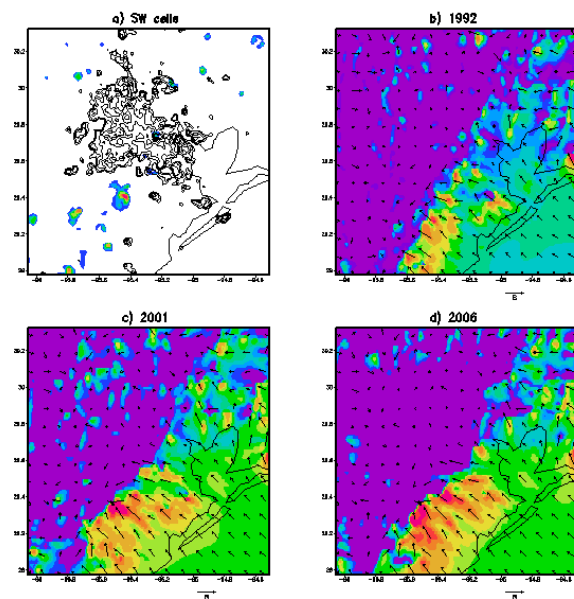


**Figure 9.** Shading in panel a indicates the position of the SW cells relative to the urban area. Comparison of the sea-breeze intensity for 1992, 2001, and 2006 runs in panels b, c, and d, respectively (shading interval = ms<sup>-1</sup>). Wind vectors at an altitude of 1 km are also plotted.

In general, when comparing experiments considering aerosol sources to the corresponding clean cities, the simulated change in the total precipitated volume was small but positive (not shown). The increase for the integral value over the finest grid was approximately 1%, however, when comparing only the cells north of the city (downwind), the simulated differences ranged from 1.7 and 9.2% for 1992, and 2006, respectively. However, the accumulated precipitation increased 10, 14 and 26%. Figure 9 shows the precipitation accumulated over grid 3 between 20:00 and 22:30 UTC and the most intense cells that we used for comparisons. When considering more polluted cities, the simulated maximum updrafts tended to be only slightly higher although they occurred at higher altitudes for all city sizes. This can be seen in Fig 10 that compares the evolution of the maximum updraft (cells in Fig 9b) for runs experiments using 1992, 2001, and 2006 land use. Left panels correspond to clean cities while the analogous runs considering urban aerosol sources are given in the right panels. The occurrence of the maxima at higher levels in linked to greater amounts of liquid water being thrust aloft into supercooled levels which then freezes releasing greater amounts of latent heat of freezing invigorating the convection. For the polluted city, supercooled mixing ratios were 15% higher than the clean case (not shown).

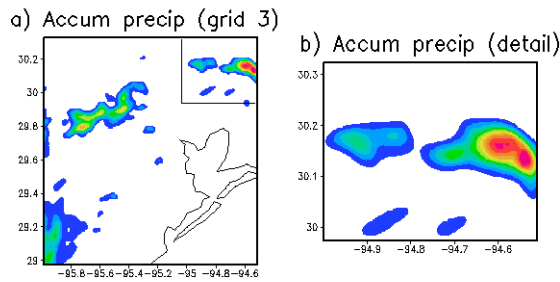


**Figure 10.** Accumulated precipitation between 20:00 and 22:00 UTC for 2001 city with no aerosol sources (a). Detail of the most intense cells (b)

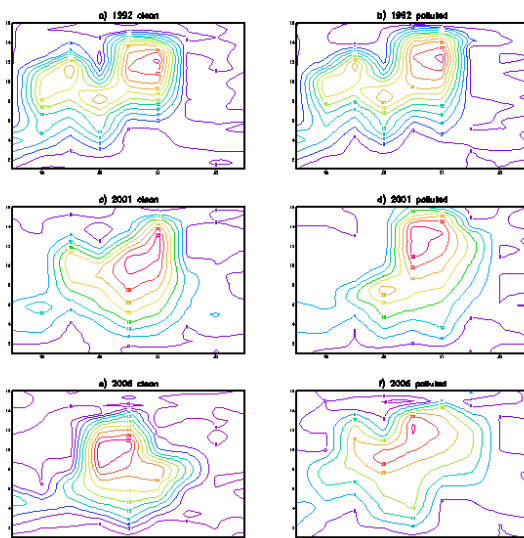


**Figure 10.** Comparison of maximum simulated updrafts. Ordinates denote altitude in kilometers and contours updrafts in  $\text{m s}^{-1}$ . Right panels correspond to clean cities and left panels correspond to CCN sources of  $2000\text{cm}^{-3}$ .

The vertical profiles of the updraft intensity and the mixing ratios of pristine ice, aggregates, rain, and the precipitating ice-phase species (hail and graupel) are compared in Fig. 11 for runs considering a clean city (2001), and different aerosol source intensities. These profiles correspond to the time the maximum updraft is attained. Updrafts maxima are slightly higher for “polluted cities” and they occur at a higher altitude. The mixing ratio of pristine ice and hail+graupel monotonically increases for more intense sources. It must be noted all sensitivity runs produced considerably higher rain mixing ratios, but the increase is *not* monotonic. Enhancing CCN concentrations leads to larger numbers of smaller drops being able to reach supercooled levels and then freezing. However, when CCN concentrations are further enhanced, the collisional mechanisms involved in the rapid

liquid-ice phase change become less efficient, a greater fraction of condensate is transported out through the storm outflow, and therefore the precipitation efficiency is reduced. The mixing ratio of aggregates exhibit a monotonic decrease when considering more intense sources, suggesting a reduced production of aggregates, a trigger for that rapid phase change.

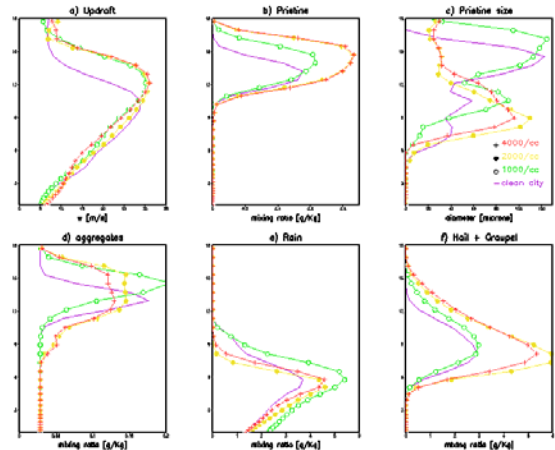


**Figure 11.** Vertical profiles at the time the maximum updraft is attained (2001 city).

All runs compared in Fig. 11 used 2001 satellite data, although these latter results are also valid for 1992 and 2006 cities (not shown).

## 5. SUMMARY AND CONCLUSIONS

We performed a series of cloud-resolving simulations to investigate the impact of the growth of city of Houston and its associated aerosol effects on convection and precipitation. The modeling framework included a detailed treatment for both, the land-use processes and the aerosol microphysics. The use of NCLD satellite data for three different years allowed an objective way to design the land-use sensitivity experiments as well as to consider the spatial distribution and differential intensities of the urban aerosol sources.

The first group of simulated storms we analyzed was virtually not affected by the urban aerosols as the sea-breeze provided a steady influx of cleaner air from the Gulf of Mexico. For these convective cells, the effects of considering larger cities can be summarized as follows. Simulated precipitation rates increased (averaged over the finest grid) with maxima occurring earlier than the NO CITY run. The total volume of precipitation (integrated over grid 3) monotonically increased from 9 to 11 to 30% (as compared to the NOCITY run) for 1992, 2001, and 2006 NCLD land use, respectively. It must be noted that the change in precipitation is *not*

related to the occurrence of more intense convective cells but to a considerable increase in the area covered by storms. For instance, the peak area coverage of these cells was 720, 870, 1000, and 1200 km<sup>2</sup> for the NO CITY, 1992, 2001, and 2006 runs, respectively, while the maximum values simulated for LPW and updraft intensity were comparable. Conversely, stronger downdrafts were simulated for numerical experiments using NLCD data. The enhanced intensity of the sea-breeze for larger urban area appears to be the main mechanism triggering the aforementioned differences between runs. Finally, larger cities (with no aerosol effects) also produced higher precipitation rates and accumulated values for urban cells although differences were relatively less important.

The second group of cells occurred within the simulated plume of pollutants. When comparing runs considering aerosol sources of different intensities, the differences in the total precipitated volume integrated over the finest grid were very almost negligible. However, the simulated maximum accumulated precipitation increased up to 26% with respect to the corresponding clean city. If we focus on the most intense convective cells, updraft maxima simulated for all numerical experiments considering aerosol sources were higher in magnitude and occurred at a higher altitude (compared to the NO CITY run). However, varying the intensity of the urban aerosol sources did not have a significant impact on the simulated updraft maxima. In agreement with previous studies mentioned in Section 1, enhancing CCN concentrations reduced the size of the liquid particles and increased the probability of liquid particles to reach supercooled levels without experiencing binary interactions. Therefore, convective cells were intensified by an additional release of latent heat. It is well known that presence of supercooled liquid water within the layer with temperatures between -10 and -20°C plays an important role in non-inductive charge separation mechanisms. The simulated liquid water masses were 4 and 9% higher than the value corresponding to a clean city, suggesting increased electrical activity.

It is important to note that the corresponding effect of this intensification on precipitation is *not* monotonic and the results of the present study explain this behavior. The efficiency of the collisional mechanisms responsible for rapid liquid-ice phase is also reduced when aerosol concentrations are further enhanced. Therefore, a greater fraction of the ice-phase condensed water mass is transported out of the storm as pristine ice crystals instead of being transferred to precipitating water species. In addition, the enhancement in the concentration of (smaller) pristine ice crystals transported to higher levels

of the storm may lead to an increase in optical thickness, area coverage and life time of the cirrus-anvil clouds (as suggested by Carrió et al. (2007)). In summary, higher pollution intensifies convective cells downwind of the city due to an additional latent heat release, although it can also reduce their precipitation efficiency by reducing the efficiency of the collision processes capable of transferring additional condensed mass at higher levels to precipitating water hydrometeors.

Finally, a non-monotonic impact on electrical activity can be expected as the charging separation mechanisms are related to the collection of supercooled droplets by graupel particles. Moreover, the relative intensification of the cells downwind of the city as well as net impact on precipitation due to urban aerosol sources may change for more or less unstable environments. For that reason, future work will focus on examining the differential impact of the Houston metropolitan area growth on sea-breeze induced convective activity characterized by different instability levels. Along that line, we are now performing a series of idealized sensitivity runs using a similar modeling framework and the August 24 2000 case as a benchmark.

## 6. ACKNOWLEDGEMENTS

The authors wish to thank NOAA (grant #NA070AR4310281) for financial support, and Athanasios Nenes and Patricia Quinn for providing and discussing aerosol data.

## 7. REFERENCES

- Carrió, G.G., S.C. van den Heever, and W.R. Cotton, 2007: Impacts of nucleating aerosol on anvil-cirrus clouds: A modeling study, *Atmos. Res.*, **84**, 111-131.
- Cotton, W. R., R.A. Pielke, Sr., R.L. Walko, G.E. Liston, C. J. Tremback, H. Jiang, R. L. McAnelly, J. Y. Harrington, M.E. Nicholls, G. G. Carrió and J. P. Mc Fadden 2003: RAMS 2001: Current Status and future directions. *Meteor. Atmos. Phys.*, **82**, 5-29.
- O'Dowd, C.D., M.E. Smith, I.E. Consterdine and J.A. Lowe, 1997: Marine aerosol, sea-salt, and the marine sulphur cycle: A short review. *Atmos. Environ.*, **31**, 73-80.
- Saleeby, S. M., and W.R. Cotton, 2004: A large-droplet model and prognostic number concentration of cloud droplets in the RAMS@CSU model. Part I: Module descriptions and Supercell test simulations. *J. Appl. Meteor.*, **43**, 182-195.